Enabling high efficiencies in MoS2 homojunction solar cells

Bueno Blanco, Carlos; Svatek, Simon Aurel; Lin, Der-Yuh; Martinez Gonzalez, Mario; Watanabe, Kenji; Taniguchi, Takashi and Antolín Fernández, Elisa

Enabling high efficiencies in MoS_2 homojunction solar cells

Carlos Bueno-Blanco[1], Simon A. Svatek[1], Der-Yuh Lin[2], Mario Martínez[1], Kenji Watanabe[3], Takashi Taniguchi[4], and Elisa Antolín[1,*]

[1] Instituto de Energía Solar, Universidad Politécnica de Madrid, Madrid 28040, Spain.

[2] Department of Electronics Engineering,National Changua University of Education, Changua 50007 Taiwan.

[3] Research Center for Functional Materials, National Institute for Materials Science,1-1 Namiki, Tsukuba 305-0044, Japan.

[4] International Center for Materials Nanoarchitectonics, National Institute for Materials Science, 1-1 Namiki, Tsukuba 305-0044, Japan.

[*] elisa.antolin@upm.es

Abstract— Van der Waals structures made of layered semiconductor materials, such as transition metal dichalcogenides (TMDCs), have been proposed for the development of ultra-thin solar cells. The performance of these devices was initially limited by low open-circuit voltages (V_{OC}), a problem that has been recently overcome with the demonstration of a V_{OC} of 1 V in a MoS_2 homojunction. However, the conversion efficiency of that proof-of-concept device was still limited, especially by the quality of the metal/semiconductor contacts. It was found that in this type of solar cells the presence of photoactive Schottky barriers at the contacts reduces the V_{OC} and the fill factor (FF). Also, MoS_2 homojunctions suffer from high reflectance at the front surface due to the large refractive index of this material. Here we present two MoS_2 homojunctions, one with metallic contacts deposited onto the MoS_2 flakes, and the second with the flakes placed onto pre-patterned contacts. We demonstrate that it is possible to achieve ideal contacts that follow the Schottky-Mott rule in the second case if the metal is deposited with a photolithography process that produces perfectly flat surfaces. We also show that light absorption in MoS_2 homojunction solar cells can be significantly enhanced by introducing a hexagonal boron nitride (h-BN) top layer.

Keywords—2D Materials, layered materials, transition metal dichalcogenides, van der Waals structures, Schottky contact, homojunction, ultra-thin solar cells.

I. INTRODUCTION

Layered TMDCs are attractive for photovoltaic applications due to their strong light-matter interaction and their simple handling. Their structure is composed by multiple layers weakly bonded through van der Waals forces. Because of the weakness of these joining forces, layered materials can be easily exfoliated. Then, devices such as *p-n* junctions can be readily built by stacking layers of different materials.

Different ultra-thin solar cells based on layered materials have been reported in the literature. The use of WSe_2 together with MoS_2 in a heterojunction produces devices able to interact with light considerably [1], [2]. However, despite showing a high photocurrent for their thickness, none of those heterojunction devices provided V_{OC} values over 0.55 V, which is a low value compared to the material band gap energies (1.2 and 1.9 eV for MoS_2 in bulk form and monolayer, respectively; 1.2 and 1.7 eV in the case of WSe_2) [3].

The use of homojunctions based on MoS_2 instead of heterojunctions produces a more favorable band alignment that enables higher V_{OC} values than the WSe_2-MoS_2 heterojunction. A V_{OC} of 1 V under an illumination equivalent to 40 suns has been demonstrated in a MoS_2 homojunction [4]. However, the performance, particularly de FF, of that device is limited because of the presence of Schottky barriers at the MoS_2/metal interface in the contacts. Also, it can only achieve a high V_{OC} in four-wire measurements and with no illumination on the contact

This work has been funded by the Spanish Ministry of Science and Innovation under Grant TEC2017-92424-EXP, by Fundación Ramón Areces within the research project SuGaR and by Comunidad de Madrid through the Madrid-PV2 Project (S2018/EMT-4308). C.B-B is grateful to Universidad Politécnica de Madrid for funding through the Predoctoral Grant Programme. M.M. acknowledges a Formación del Personal Investigador Predoctoral Fellowship (PRE2019-087894) and E.A. acknowledges a Ramón y Cajal Fellowship (RYC-2015-18539), both funded by the Spanish Ministry of Science and Innovation.

area (because the Schottky barriers are photoactive and their photogeneration reduces the V_{OC} of the device). In the same study it was estimated that eliminating the Schottky barriers at the contacts would raise the efficiency from 2% to~6%.

It this work we present two MoS_2 homojunction where the Schottky barriers have been mitigated by an appropriate selection of metals for the electrical contacts. In the first one, the metals are deposited onto the MoS_2 surface, and on the second one the MoS_2 flakes have been deposited onto pre-patterned metal contacts. In the first case the Schottky barriers are only mitigated, whereas in the second case we achieve perfectly ohmic contacts. When using pre-patterned contacts, we show the importance of achieving a flat and spotless metal surface in order to allow the semiconductor to adapt correctly to the shape of the pad. Furthermore, we show that the addition of an anti-reflection layer (ARL) of h-BN increases the absorption of the devices, enhancing their photocurrent.

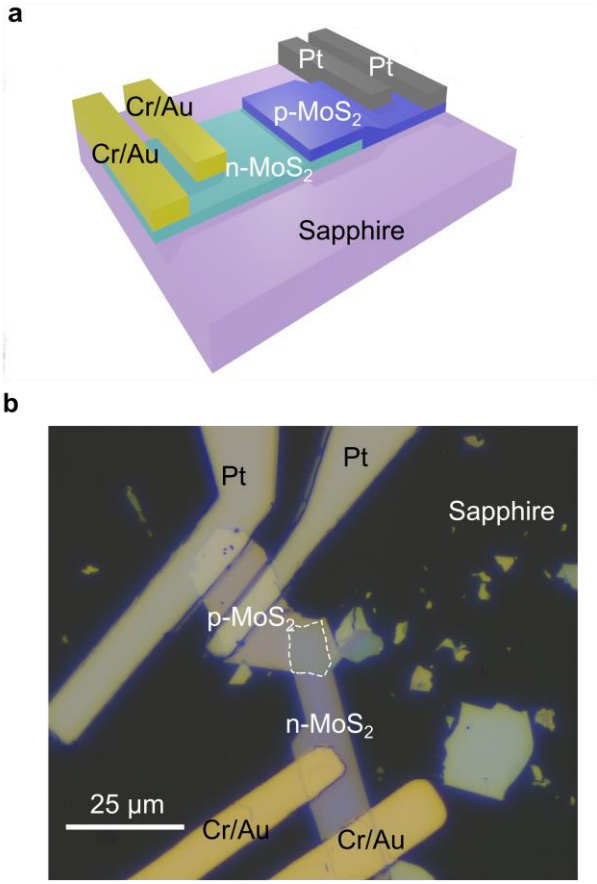

Fig. 1: Schematic (a) and micrograph (b) of a MoS_2 homojunction device with metal contacts deposited on top of the semiconductor flakes.

II. *P-N* Homojunction and the Importance of the Contact Tehcnology

MoS_2 is naturally an *n*-type semiconductor. Here we have used *n*-MoS_2 doped with 0.5% Fe and a stable *p*-type MoS_2 produced using Nb as substitutional dopant also in a 0.5% concentration [5].

The method to build the MoS_2 *p-n* homojunctions is explained in our previous work [4]. It has been adapted from the hot pick-up technique [6]. Semiconductors are directly exfoliated from a bulk fresh crystal onto a SiO_2/Si substrate. The flakes are picked with a PDMS (Polydimethylsiloxane) stamp coated with PPC (Polypropylene carbonate) at 45 ºC building the *p-n* junction on the stamp. Then, they are deposited onto a sapphire substrate and the substrate is heated to 95ºC to detach the PPC from the PDMS stamp. Following this step, PPC residues are removed using chloroform. In our first device, after releasing the *p-n* junction on the substrate, metal contacts are deposited using maskless photolithography and a physical vapor deposition (PVD) technique. Four electrical contacts are made, two for each flake, using platinum for the *p*-material (deposited by sputtering) and chromium for the *n*-material (deposited by thermal evaporation). The resulting device has the structure represented in Fig. 1a. A micrograph is shown in Fig. 1b. The thicknesses are 45 nm for the *p*-MoS_2 flake and 60 nm for the *n*-MoS_2 flake, as measured by atomic force microscopy (AFM).

The thickness of TMDCs layers in ultra-thin solar cells are frequently under 60 nm. Unlike bulk devices, TMDC-based devices are so thin that there is no chance of introducing a highly doped buffer layer between semiconductor and metal that facilitates an effective ohmic contact. This feature makes ultra-thin solar cells different from conventional ones because the band alignment between metal and semiconductor must be correct to obtain an ohmic contact. The choice of metal for each contact is based on the metal work function [7]. Pt, with a work function of 5.6 eV, is a good choice for contacting the *p*-material (valence band maximum at 5.6 eV). For the *n*-material, a low work function metal should be selected (the conduction band minimum is at 4.2 eV). Cr is a good choice for this contact with a work function of 4.5 eV [8]. The Cr surface is coated with a gold layer to avoid oxidation and facilitate the measurement of the device.

To improve the contact adhesion, the device is annealed at 100 ºC for 30 min. As we have two terminals on each flake, it is possible to measure each TMDC/metal contact individually to check if it is ohmic. Fig. 2 shows the current density-voltage (*J-V*) characteristics measured between the two contacts of the *n*-MoS_2 flake and between the two contacts of the *p*-MoS_2 flake under illumination with a broad-band light source (they are tested under illumination because if a Schottky barrier is present, it can be photoactive). The *n*-contact is perfectly ohmic and shows a high conductivity. The *p*-side shows a non-ohmic behavior. Still, the conductivity in the current density range that is useful for photovoltaic applications is high enough to produce acceptable losses in a proof-of-concept device.

During the thermal deposition process, the surface of semiconductors could be affected. There is a difference in the process of fabrication of both contacts. Cr contacts are implemented by thermal evaporation whereas Pt contacts are made by sputtering. Sputtering process involves the use of plasma that can be more aggressive than conventional thermal evaporation. Therefore, Pt deposition is more susceptible to damage the semiconductor affecting the quality of the contact.

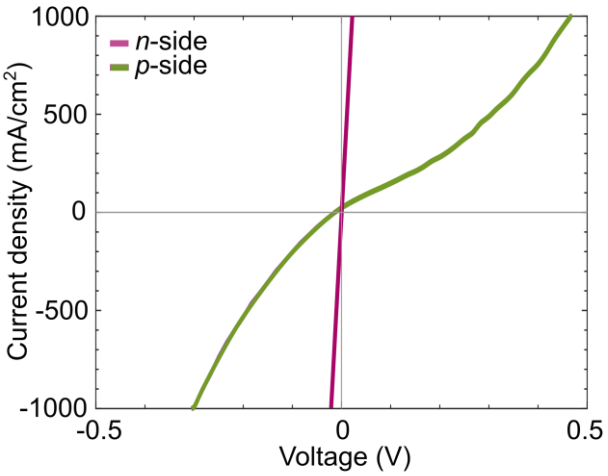

Fig 2. *J-V* curves measured between the two contact pads of each flake under broadband illumination with 4 W/cm^2 to test the metal/semiconductor contacts. The *n*-MoS_2-Cr contact in purple and the *p*-MoS_2-Pt contact in green.

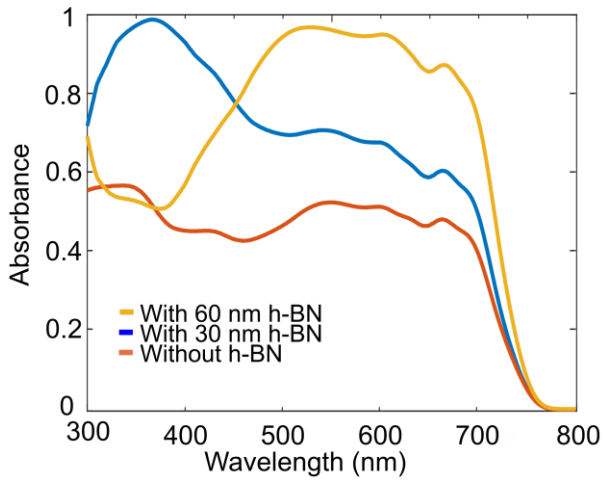

Fig. 3. Modeled absorbance for a 105 nm MoS_2 layer over a 500 µm sapphire substrate without h-BN ARL (orange), with a 30 nm h-BN ARL (blue) or with a 60 nm h-BN ARL (yellow).

III. Improving Device Absorption

To increase the photocurrent of these ultra-thin solar cells it is necessary to maximize the optical absorption. The main optical loss in a MoS_2 homojunction device with thickness in the 100 nm range is the strong front surface reflection, which results from the high refractive index of MoS_2 [4]. To reduce the reflection, an ARL can be added, which should have a refractive index close to the geometrical mean of the indexes of MoS_2 and air. h-BN is a good candidate to fabricate an ARL because it has a suitable refractive index, and it is a layered material that can be easily stacked onto the *p-n* junction using the pick-up technique described above. Besides, h-BN has been reported to passivate the surfaces of 2D materials and improve their optoelectronic properties [9].

We have calculated the optical absorption of the device using the transfer matrix method [10]. With this method it is possible to calculate the light flux in each layer of a multilayer structure, from a matrix whose elements are obtained from the Fresnel equations for each material and each interface. Fig. 3 shows the absorbance of a 105 nm think MoS_2 layer over a 500 µm sapphire substrate with no h-BN ARL (orange), with a 30 nm h-BN flake (blue) and with a 60 nm h-BN flake (yellow). The calculations with the h-BN ARL show a higher absorbance, especially in the case of the 60 nm flake. By integrating the product of the absorbance and the AM1.5G spectrum, we estimate that the addition of a 30 nm-thick h-BN ARL increases the one-sun photocurrent by a factor of 1.5, and by 1.75 if the ARL is 60 nm thick. Although a thinner h-BN layer enhances the absorption in the ultraviolet range, a thicker h-BN improves the absorption in the visible range, where the AM1.5G spectrum has a higher number of photons.

We have tested the effect of the h-BN ARL on the device shown in Fig. 1. Fig. 4 shows micrographs of the device before and after depositing a 30 nm thick h-BN flake that covers the whole p-n junction. *J-V* curves measured before and after adding the 30 nm h-BN ARL are presented in Fig 4.b. They have been measured under a broadband illumination (halogen lamp) with 4 W/cm^2 power density.

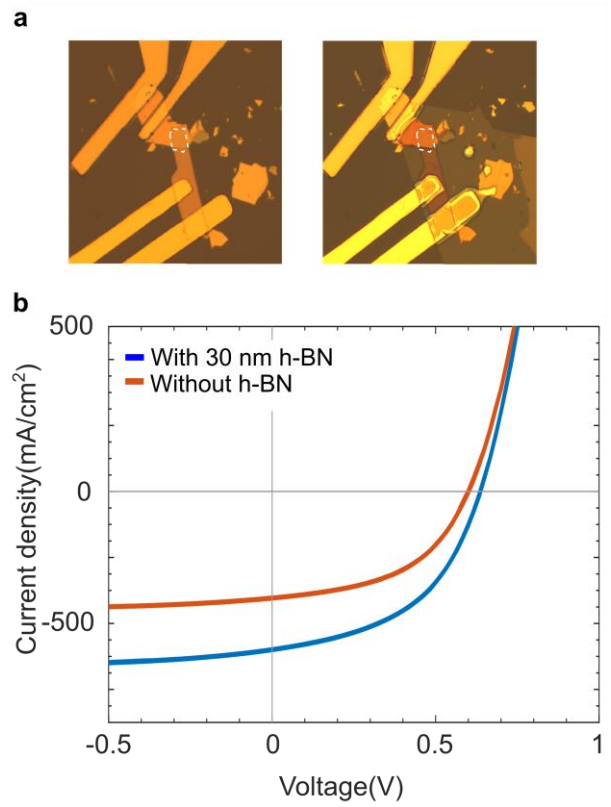

Fig 4 (a) Micrographs of the MoS_2 homojunction device before (left) and after (right) depositing the h-BN flake. (b) *J-V* curves of the device under broadband light with 4 W/cm^2 power density, before (red) and after (blue) placing the h-BN.

The FF of the *J-V* curves is 48%, significantly better than previous results [4]. Notice also that these curves were measured with illumination on the whole chip, and they do not show the detrimental contribution of photoactive Schottky barriers at the contacts. Also, the comparison between the blue and red curves shows that the short-circuit current density increases by almost a 1.5 factor after the deposition of the 30 nm thick h-BN flake, in agreement with the theoretical model. Also, the photocurrent

enhancement produces a slight increase in the V_{OC}, as expected from the superposition principle.

IV. IMPROVING THE METAL-SEMICONDUCTOR INTERFACE

In the device presented previously, the metallic contacts are directly evaporated onto the previously built *p-n* junction. Although the *J-V* curve from Fig 2 for the *n*-MoS_2-Cr contact is ohmic, this is not the case of the *p*-MoS_2 pair. According to the Schottky-Mott rule, platinum should make an ohmic contact to *p*-MoS_2 as its work function matches the maximum of the MoS_2 valence band. We find the following explanation has been proposed for this phenomenon [11]. 2D materials are characterized by having autopassivated surfaces with no dangling bonds. However, when metals are deposited on the semiconductors, metal atoms hit the surface of the semiconductor breaking the continuity of the lattice and generating defects. Because of these defects, an intermediate energy level is generated so the properties of the metal/semiconductor contact are no longer dependent on the metal work function, inducing a Fermi level pinning Consequently, the Schottky-Mott rule is not useful to predict the band alignment [12]. A schematic of what is happening during the PVD process is depicted in Fig 5.a.

Our approach to overcome this problem is to change the structure of the device and look for a defect-free interface between semiconductor and metal. Liu *et al.* [12] have reported TMDC/ metal contacts that fulfil the Schottky-Mott rule obtained by transferring the metal onto the semiconductor flake with a polymer stamp. However, the process involves several steps where metal pads are peeled and transferred, making it hard and costly. Here we present a simpler technique. Instead of transferring the metal, the semiconductor flakes will be transferred onto pre-patterned metal pads as it is presented in Fig 5.b. Metal pads are fabricated using a maskless photolithography process (SmartPrint). We have found that the fabrication technique of these metal pads is critical for the achievement of ideal metal/semiconductor contacts.

Fig 6.a shows the process flow of a standard contact fabrication.. A negative photoresist, AZ1512 HS is spun over the surface of the substrate and baked at 100ºC for two minutes. After this step, the substrate is exposed selectively to ultraviolet light in order to create a specific pattern over the photoresist. The exposed photoresist is removed with devoloper, the metal is deposited by PVD, and the remaining photoresist is cleaned off with organic solvents. We find that this method, which is sufficient for conventional solar cells, produces defects that can be detrimental for the metal/semiconductor interface in our application. During the metal deposition, the material tends to deposit on the borders of the pads. The accumulation of leftover material results in defective borders as shown Fig 6.a. The semiconductor flakes cannot adapt to the steep edges of the metallic pads, and they come into contact with the metal only in few points generating hot spots. As a result of this, devices degrade under current flow. Fig 7.a shows a schematic of a semiconductor layer on defective contacts and in Fig 7.b there is an example of MoS_2 homojunction where the semiconductor is burnt because of the current concentration on hot spots at the metal borders.

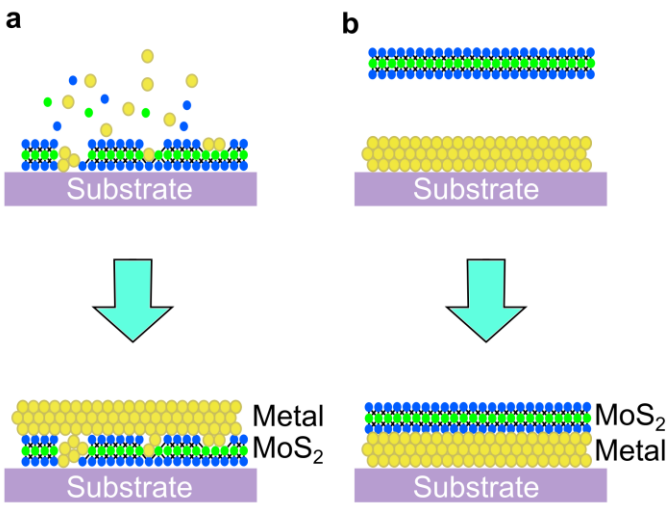

Fig 5. Atomic disposition of metal and MoS_2. (a) Metal deposition by PVD onto previously placed MoS_2. (b) MoS_2 transferred onto a pre-patterned metal pad.

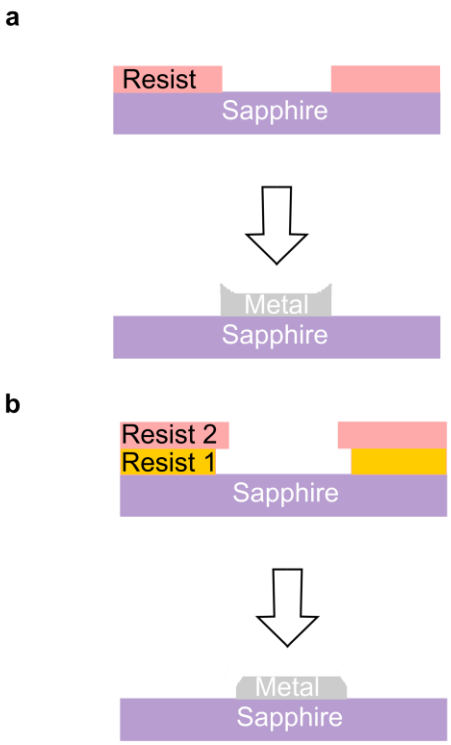

Fig 6. Schematic of photolithography processes(a) Single-layer resist process. (b) bilayer resist process.

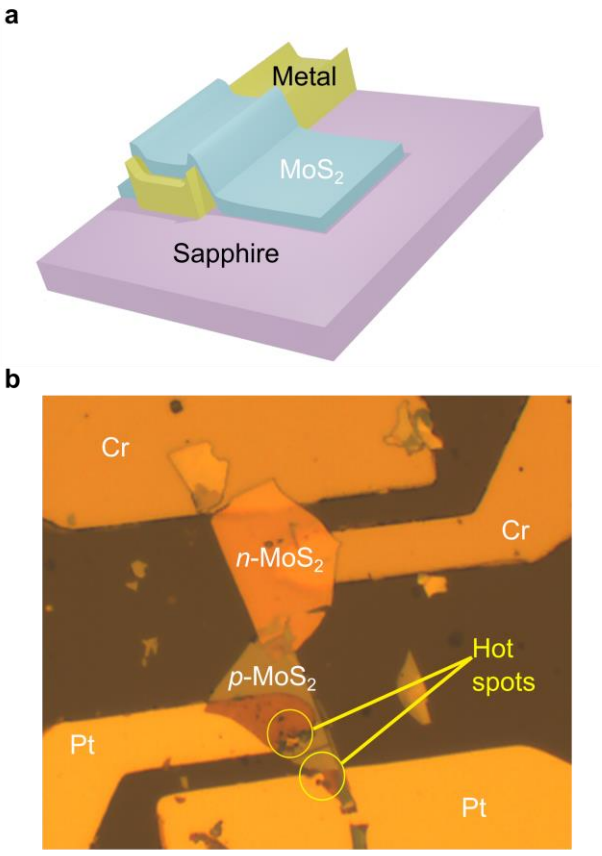

Fig 7. (a) Schematic of MoS_2 on non-ideal metal pads. (b) MoS_2 homojunction on non-ideal metal pads: current flow at the hot spots on the borders destroys the semiconductor.

The accumulation of leftover material caused by photolithography can be avoided by adding an additional step to this process. Fig 6 shows the results of two processes of photolithography, in Fig.6.a the conventional one and in Fig 6.b an alternative which implies the use of two photoresists. These two photoresists are the previously mentioned A1512HS used as top resist, and the LOR7B which is the bottom one. LOR7B is spun and baked at 180ºC for three minutes and after that, AZ1512HS is spun and baked at 100ºC for two minutes. LOR7B resist is more sensitive to the light so that, when both are exposed, the bottom one is affected in a larger area developing an undercut once both resists are removed with a developer, as it can be appreciated in Fig 7.b. The presence of this undercut allows the metal to deposit under the top photoresist without sticking to the borders of the pattern. Fig. 8 shows the comparison between two metallic contacts created either by simple photolithography or by bilayer photolithography, along with their respective profiles measured by AFM. In Fig 8.b, it is visible that the accumulation of metal at the border results in steep edges, which would force the flakes to bend excessively to follow the morphology of the pads. In Fig 8.d, it is appreciable that the bilayer resist process produces smoother borders that can allow the semiconductor to perfectly stick to the metal surface.

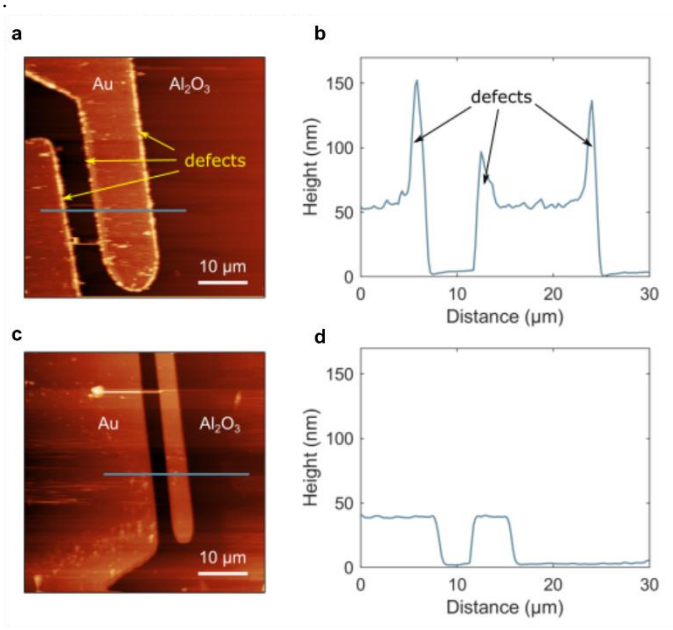

Fig 8. AFM characterization comparing single-resist and double-resist fabrication processes. (a) Topography scan on pre-patterned contacts fabricated with single layer. (b) Profile along the blue line shown in a. (c) Topography scan on pre-patterned contacts fabricated with bilayer resist. (d) Profile along the blue line shown in c.

V. Ohmic Contacts to 2D Materials

In Section II we have presented *J-V* curves of metal/semiconductor junctions showing an ohmic contact for the *n*-MoS_2 with chromium, while the junction between *p*-MoS_2 and platinum is clearly less conductive. According to the Schottky-Mott rule, both metals should make an ohmic contact, but this is not the case of the *p*-MoS_2-Pt combination, because of the defects caused by the thermal deposition process.

With the implementation of bilayer-resist photolithography and by building the device over already fabricated metal pads, a perfect physical contact between metal and semiconductor can be obtained as depicted in Fig 9.a, which enables a contact behavior following the Schottky-Mott rule. Fig 9.b and Fig 9.c show two devices in which a flake of semiconductor has been deposited between two electrical contacts made of Cr for *n*-MoS_2 and made of Pt for *p*-MoS_2, both fabricated using bilayer resist. The *J-V* curve for each device is plotted in Fig 9.d.

In this case, both *J-V* curves are as predicted by the Schottky-Mott rule However, the Cr contact can be problematic as this metal develops an oxide passivating layer in air that damages the quality of the contact. We have found that keeping the pre-made metal pads are kept in a N_2 atmosphere until the semiconductor flakes are deposited preserves the surface free of oxide and allows us to achieve a good electrical contact. The fabrication procedure presented here produces metal/TMDC contacts of quality comparable to the ones reported in [12] with a process that is more robust and easier to implement.

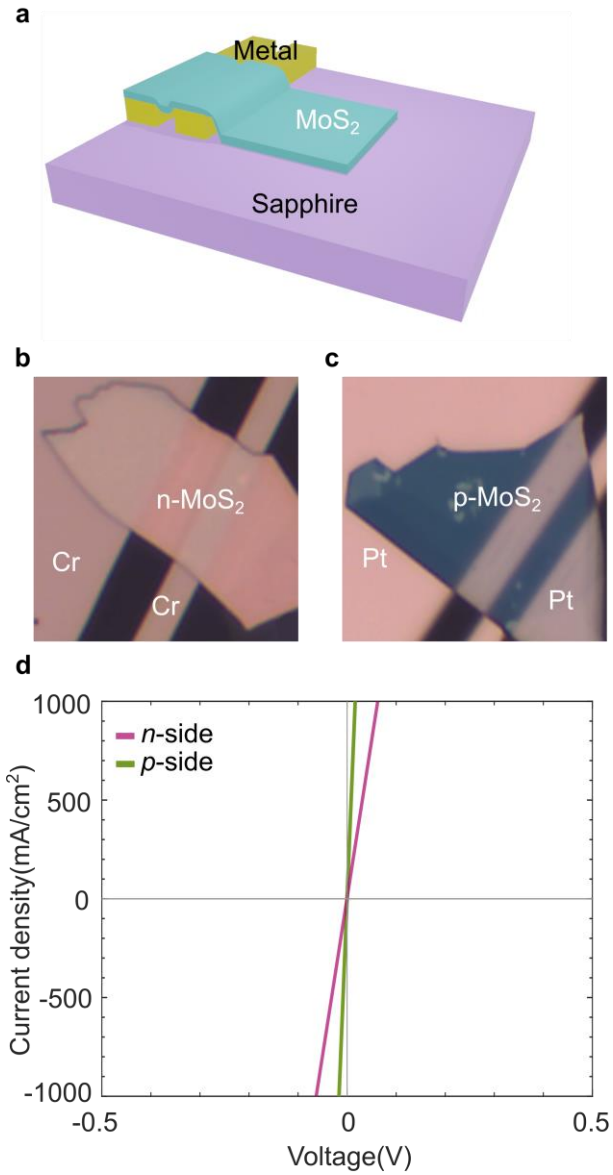

Fig 9. (a) Schematic of a MoS_2 flake on perfectly flat pre-patterned metallic surfaces. (b) Micrograph of *n*-MoS_2 flake on chromium contacts. (c) Micrograph of *p*-MoS_2 flake on platinum contacts. (d) *J-V* curve of both metal/semiconductor contacts under illumination with a broadband 4 W/cm^2 source, purple Cr-n-MoS2 and green Pt-p-MoS2.

VI. Conclusions

We have demonstrated the fabrication of metallic contacts to MoS_2 homojunctions with reduced Schottky barriers or total absence of Schottky barriers, and the implementation of an h-BN ARL to enhance their photocurrent. We have developed a fabrication process that produces perfectly ohmic contacts to *n* and *p*-doped MoS_2 by: (i) choosing metals of specific work function (Cr and Pt, respectively), (ii) fabricating perfectly flat metal pads with a bilayer resist, and (iii) depositing the flakes onto the pre-patterned contacts. This process is easier and faster that the procedure previously reported, as metal transfer from polymer stamps is avoided. These results pave the way for the achievement of high efficiencies in the emerging technology TMDC-based ultra-thin, ultra-light solar cells.

Acknowledgments

The authors would like to thank Irene Artacho and Miguel Gómez for technical support.

References

[1] C.-H. Lee *et al.*, «Atomically thin p–n junctions with van der Waals heterointerfaces», Nat. Nanotechnol., vol. 9, n.º 9, Art. n.º 9, sep. 2014, doi: 10.1038/nnano.2014.150.

[2] J. Wong *et al.*, «High Photovoltaic Quantum Efficiency in Ultrathin van der Waals Heterostructures», ACS Nano, vol. 11, n.º 7, pp. 7230-7240, jul. 2017, doi: 10.1021/acsnano.7b03148.

[3] J. Gusakova *et al.*, «Electronic Properties of Bulk and Monolayer TMDs: Theoretical Study Within DFT Framework (GVJ-2e Method)», Phys. Status Solidi *A*, vol. 214, n.º 12, p. 1700218, 2017, doi: https://doi.org/10.1002/pssa.201700218.

[4] S. A. Svatek *et al.*, «High open-circuit voltage in transition metal dichalcogenide solar cells», Nano Energy, vol. 79, p. 105427, jan. 2021, doi: 10.1016/j.nanoen.2020.105427.

[5] J. Suh *et al.*, «Doping against the Native Propensity of MoS2: Degenerate Hole Doping by Cation Substitution», Nano Lett., vol. 14, n.º 12, pp. 6976-6982, dec. 2014, doi: 10.1021/nl503251h.

[6] F. Pizzocchero *et al.*, «The hot pick-up technique for batch assembly of van der Waals heterostructures», *N*at. Commun., vol. 7, n.º 1, Art. n.º 1, jun. 2016, doi: 10.1038/ncomms11894.

[7] L. Wang *et al.*, «One-Dimensional Electrical Contact to a Two-Dimensional Material», Science, vol. 342, n.º 6158, pp. 614-617, nov. 2013, doi: 10.1126/science.1244358.

[8] D. S. Schulman, A. J. Arnold, y S. Das, «Contact engineering for 2D materials and devices», Chem. Soc. Rev., vol. 47, n.º 9, pp. 3037-3058, may 2018, doi: 10.1039/C7CS00828G.

[9] Z. Yang *et al.*, «A Fermi-Level-Pinning-Free 1D Electrical Contact at the Intrinsic 2D MoS2–Metal Junction», Adv. Mater., vol. 31, n.º 25, p. 1808231, 2019, doi: https://doi.org/10.1002/adma.201808231.

[10] E. Centurioni, «Generalized matrix method for calculation of internal light energy flux in mixed coherent and incoherent multilayers», Appl. Opt., vol. 44, n.º 35, pp. 7532-7539, dec. 2005, doi: 10.1364/AO.44.007532.

[11] C. Kim *et al.*, «Fermi Level Pinning at Electrical Metal Contacts of Monolayer Molybdenum Dichalcogenides», ACS Nano, vol. 11, n.º 2, pp. 1588-1596, feb. 2017, doi: 10.1021/acsnano.6b07159.

[12] Y. Liu *et al.*, «Approaching the Schottky–Mott limit in van der Waals metal–semiconductor junctions», Nature, vol. 557, n.º 7707, Art. n.º 7707, may 2018, doi: 10.1038/s41586-018-0129-8.